VOL. 6, NO. 7, JULY 2011 ISSN 1819-6608
ARPN Journal of Engineering and Applied Sciences


www.arpnjournals.com

EXPERIMENTAL STUDY FOR HEAT AND MASS TRANSFER FROM MOIST AIR FLOWING OVER MOVING WATER FILM

Ahmed F. Khudheyer
Department of Mechanical Engineering, Al-Nahrain University, Baghdad, Iraq
E-Mail: ahyaja@yahoo.com

ABSTRACT

Heat and mass transfer from or to a horizontal moving water film to airflow flowing over the film inside a rectangular duct wind tunnel is investigated, experimentally. To perform the experimental study for this phenomenon air flows inside a rectangular duct over a moving water film flow inside the duct, which is fixed in the floor of the tunnel. Therefore, some of the water film is evaporated from the water surface to the air flowing over it. The following measurements for velocity of moist air and water, temperature, humidity, are taken at five positions along test section and upstream of the water panel with a range of Reynolds number of (1000-30000). Also, the amount of water evaporated through each experiment is measured. The results show that, Nusselt and Sherwood numbers increase with increasing Reynolds number. Comparison between the obtained results and the previous works show good agreement.

Keywords: heat and mass transfer, moist air, moving water film.

1. INTRODUCTION

The evaporation of a liquid into a gas consisting of its own vapour, air or a mixture is important in many chemical and industrial engineering processes. The gas can be considered as a binary mixture. In the present study, the coupled heat and mass transfer describing this process are set up and solved for a range of gas temperatures and compositions. The calculations are carried out at atmospheric pressure using air as the inner gas and water as the evaporating liquid, which represents a common case in drying. The results of these calculations are the evaporation rates. With the knowledge of these, the so-called inversion temperature can be determined. The inversion temperature has most commonly been described as the gas temperature at which the evaporation rate is decrease.

Heat and mass transfer processes through air-water interface are of major importance in many engineering applications. Such that, an analysis from an air-water interface is of particular interest for water thermal pollution control where, an air stream flowing parallel to surface of water or river is used to dissipate heat. Mass transfer problems involving phase change, like evaporation must also involve heat transfer, and the solution needs to be analyzed by considering simultaneous heat and mass transfer. Some examples of simultaneous heat and mass transfer are drying, evaporative cooling, transpiration cooling, combustion of fuel droplets, cooling by dry ice …etc. To explain the mechanism of simultaneous heat and mass transfer, consider the evaporation of water from a pool into air. The evaporation of water and the diffusion of this vapor into the flowing air require the transfer of the latent heat of vaporization to the water in order to vaporize it. Therefore, combined heat and mass transfer processes that occur when water evaporates into air.

Heat and mass transfer govern the process of evaporation from a water surface into airflow. The boundary layer incorporates a resistance for both heat and mass transport processes. At low temperatures the process is mainly heat transfer controlled, since the concentration difference across the boundary layer is large as compared to a rather small temperature difference. At low temperature difference, the required heat for vaporization of water at the surface to the flowing air is transferred by convection from the flowing air stream and by conduction from the water under the surface due to the sensible heat of the water itself. With increasing gas temperature the temperature difference between the surface and gas, and consequently, the heat transfer rate increases. The concentration difference increases as well because of the combined increase in temperature and saturation pressure at interface. While the increase of the temperature difference is unlimited, the concentration difference reaches a maximum when the interface saturation pressure reaches the pressure of the system. Consequently, the whole process of evaporation becomes mass transfer controlled and the mass transfer resistance is the governing factor.

In pure superheated steam the mass transfer resistance does not exist, since the gas consists only of the evaporating species. This explains why the evaporation into pure superheated vapor is greater than into dry air at higher temperatures.

In most of the engineering applications, heat and mass transfer occur simultaneously and often these are strongly coupled. A comprehensive analysis of simultaneous heat and mass transfer from a gas-liquid interface has not been found in the available literature. The evaporation of liquids in air is important in heat and mass transfer and exists in different industrial applications such as drying, air conditioning and desalting. The case of evaporation of water by superheated steam has also received considerable attention in many experimental studies. Because the using of the superheated vapour steam as drying medium is recommended for drying materials that are sensitive to oxidation and sensitive temperature such as food products.

Evaporation of liquid into its own vapor, air and mixture there is a problem of coupled heat and mass transfer, which studied by:

Eames *et al*., (1997) has collected a review on the evaporation coefficient of water. It is concluded that, molecular collision in the vapor phase and heat transfer limitation in the liquid phase can have a considerable influence on experimental evaporation rates.

Combined heat and mass transfer processes that occur when water evaporates from a flowing film in an inclined channel to air stream, have been investigated by Zheng and Worek (1996). It was found that the combined heat and mass transfer in film evaporation can be enhanced by adding rods to the plate surface to agitate mechanically the flowing water film and air stream.

G. Grossman and K. Gommed, (1997) studied heat and mass transfer in film absorption in the presence of non - absorption gases. The effect of non-absorbable gases on the simultaneous heat and mass transfer process in film absorption has been analyzed. A reduction in mass flux is caused by the presence of these gases in the gas phase. When the latter is large compared to the resistance in the liquid, even minute quantities of non- absorbable gas, can cause a considerable deterioration. Initial mass fraction of non-absorbable, the lower the mass flux. The smaller the heat of absorption and the larger the pressure driving force, the greater the mass flux as in the absence of non-absorbable.

Kuan-Tzong Lee, (1998) studied mixed convection heat transfer in horizontal rectangular ducts with wall transpiration effects. A detailed numerical study was carried out to examine the effects of wall transpiration on laminar mixed convection flow and heat transfer in the entrance region of horizontal rectangular ducts. The vorticity velocity method was employed in the formulation of both thermal boundary condition of uniform heat flux and uniform wall temperature. Predicted result was presented for airflow over a wide range of governing parameters. In this work the wall Reynolds number are varied from -2 (suction) to 4 (injection) and Rayleigh number was ranging from 0.0 to $2x10^5$ for aspect ratio (0.2, 0.5, 1.2 and 5).

M. Haji and L. C. Chow (1988) studied heat and mass transfer with dehumidification in laminar boundary layer flow along a cooled flat plate. The effects of dehumidification, from laminar flow humid air, over isothermal cooled flat plate have been investigated using the similarity principle. The results obtained for both saturated and unsaturated humid air is compared with those of dry air. It can be concluded that dehumidification has a significant effect of both sensible and latent heat transfer as well as the friction factor. However, the difference in heat transfer coefficient of humid and dry air is reduced as the relative humidity is decreased.

Wel-mon Yan, (1995) studied transport phenomena of developing laminar mixed convection heat and mass transfer in inclined rectangular ducts. The developing laminar mixed convection heat and mass transfer in inclined rectangular ducts has been studied numerically, with six independent parameters; Prandtl number Pr, mixed convection parameter (Pr Gr/Re), modified Rayleigh number Ra*, buoyancy ratio N, Schmidt number Sc and aspect ratio. Typical developments of velocity, temperature and concentration profiles are shown to include the limiting cases of horizontal and vertical rectangular ducts. Sheikholeslami and Watkinson (1992) examined the effect of steam content on the rate of evaporation of water into moist air and superheated steam at elevated temperatures. Their experimental results confirmed the existence of inversion point temperature, above which the rate of evaporation of water increases with increasing in the steam content of the medium.

The experiments reported by Sparrow and Tao (1983) were performed in a flat rectangular duct to determine the mass (heat) transfer and pressure drop response to periodic, rod-type disturbance elements situated adjacent to one of the principal wall and oriented transverse to the flow direction.

In this work, experimental study of the heat and mass transfer from water panel for moist air flow inside the tunnel at different velocities is carried out.

2. EXPERIMENTAL TEST RIG

In this section, a description of the experimental set-up is presented. The test rig is designed and constructed, such that one can investigate the effect of the operating parameters of evaporation process above horizontal cooled or heated water surface. The details of test section, experimental and calculation procedure are presented in Figures 1 and 2. The test section is designed and constructed, in gas dynamic laboratory, to study the parameters affecting the evaporation process to moist air flowing in a horizontal rectangular duct with water panel at the bottom. The test section is attached to a wind tunnel, which provides atmospheric air at different flow rates. Figure-1 shows the layout of the test rig including the designed test section. The atmospheric moist air is drawn into the tunnel by an axial fan (9), which is driven by a variable speed electric motor (8). In accordance, the mass flow rate of the tested air can be varied using the speed regulator (motor control) (7). The water flow at the bottom of the test section is controlled by flow meter an external refrigerating or heating unit (5) to heat or cool the inlet water.

The value of this temperature is controlled by thermostat. For the case of smaller values of mass flow rate, this value of temperature is adjustable using a thermostat connected to the refrigerating unit motor or heating element. A number of 10 thermocouples, Type K are used to measure the temperature of the water. All thermocouples are connected to digital temperature recorder, which has an accuracy of $\pm$ 0.1^{o}C. The steady state condition is achieved after a time period varied from 60 to 90 minutes, depending on the value of air flow rate.

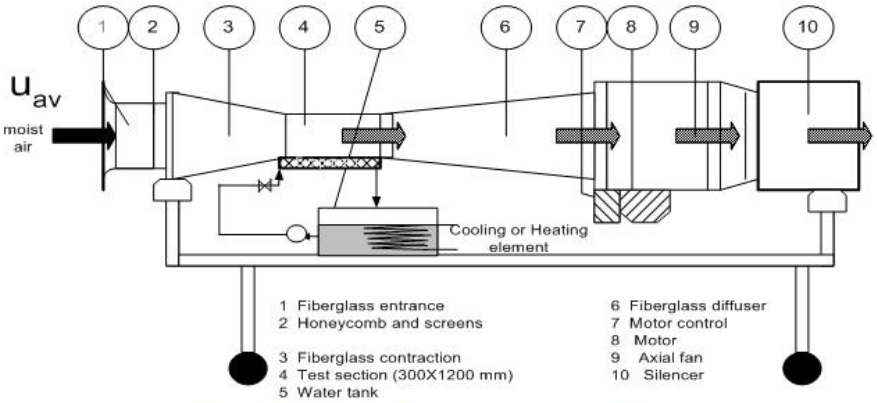

Figure-1. Schematic diagram of experimental test rig.

Test section is a rectangular duct with dimension 300×300 mm and length 1200 mm and 10 mm water panel at the bottom of the test section. Five equally space slots with dimensions (12×300 mm) each, at X= (0.0, 0.25, 0.5, 0.75, 1.0) in total length are cut in the front side. A simple transverse mechanism is consisting of the sliding ruler (11), which contains a circular - hole (12). The hygrometer (13) of accuracy ± 0.1°C mounted through this hole is used to measure the dry bulb and wet bulb temperatures at different points inside the duct.

The sliding ruler is directed up and down according to the required measuring position. A fixed plate and bolts are used to maintain the sliding ruler at the required position. The digital hygrometer is free to move in Z-directed, to ensure the possibility of measuring at different positions in Z-direction.

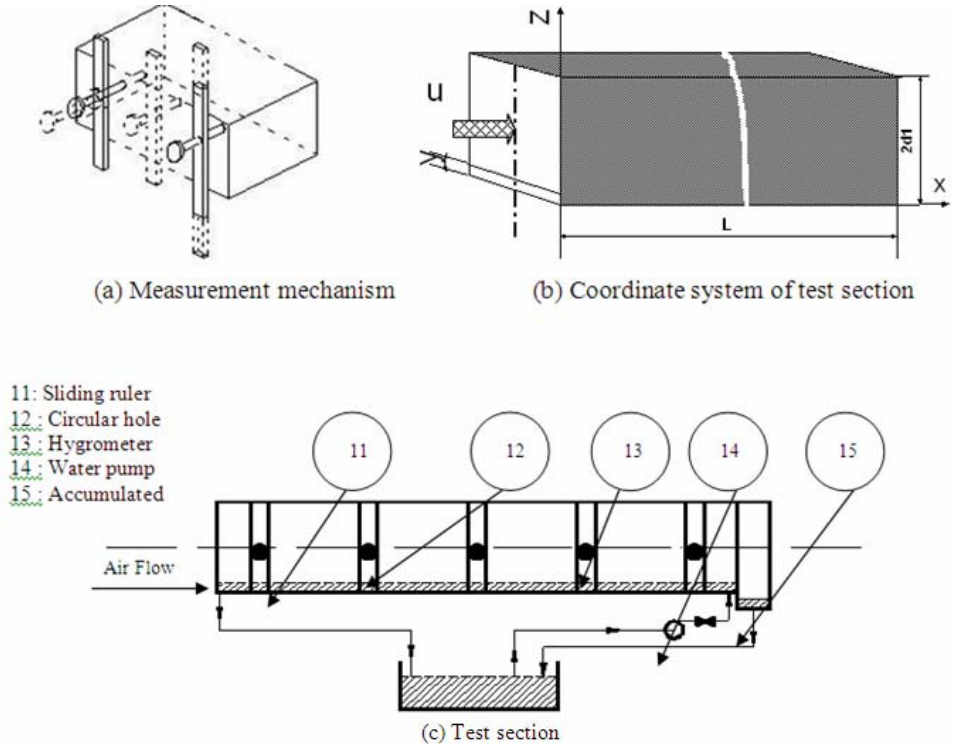

Figure-2. Details of the test section.

2.1 Experimental procedure

Before starting a new run, the test loop is adjusted for leakage of air and water. Each run is carried out for certain fixed value of the problem parameters (velocity and surrounding temperature). The experimental procedure for each run can be described in the following steps:

a) Switch on the pump to circulate cold or hot water
b) Switch on the motor of wind tunnel.
c) Adjust the frequency of motor speed of wind tunnel to obtain the desired flow rate for circulating humid air.

The humid air circulated till steady state condition is reached. The steady state condition is achieved after about 120 minute.

The following measurements are taken for each run of the experiment.

- Frequency of motor of wind tunnel (Hz)
- Temperature at water flow in panel (t_w)
- Dry bulb temperature at different section of duct
- Dbt, wet bulb temperature at different section of duct

2.2 Calculations procedure

By measuring the temperature at inlet and outlet of every section of the duct and velocity at each run, one can evaluate the local and average Nusselt number for every value of any velocity mass flow of dry air can be calculated according to the following equation:

$$\dot{m}_{air} = A_c \cdot u_{av} \cdot \rho_{air} \quad (1)$$

Where m_{air} ,ρ_{air} , A_c and u_{av} are mass flow rate of dry air , density of dry air and wind tunnel cross sectional area of duct (300x300mm^2) and average velocity of air, respectively. Using the following relations, the average heat and mass fluxes can be calculated at any segment of the test section as shown in Figure-3, which lies between two successive measuring positions (along the length of test section).

$$q'' = \frac{\dot{m}_{air}}{A_a} \cdot \Delta i \, , m'' = \frac{\dot{m}_{air}}{A_a} \cdot \Delta w \quad (2)$$

Where q'' is heat flux, m'' mass flux? $A_{a\ is}$ the surface area of the considered segment, Δi and Δw are the difference of the total enthalpy and humidity ratio between the inlet and outlet of this segment. The enthalpy i and humidity w are determined from Table sited in references [10], knowing the average dry and wet bulb temperatures at the considered section. Yet, one can calculate heat and mass transfer coefficients as follows:

$$h = q''/(T_\infty - T_w) \quad h_m = m''/(\rho_\infty - \rho_w) \quad (3)$$

Where h, h_m heat transfer coefficient, mass transfer coefficient, t_∞, dry bulb temperature for moist air far from the water film flow in the bottom, t_w water temperature, ρ_w density of saturated vapor at water temperature and ρ_∞ density of superheated vapor far from the water film in bottom.

$$p_v = RH \cdot p_s \quad (4)$$

One can calculate the ρ_v from superheated vapor table at d_{bt}, p_v we get specific volume for water vapor (v).

$$\rho_v = 1/v \quad (5)$$

Where p_v, p_s are vapor pressure, and saturated vapor pressure respectively, RH is the relative humidity and ρ_v is the density of superheated vapor

Accordingly, one can calculate local Reynolds, Nusselt and Sherwood numbers as;

$$\mathrm{Re} = .\frac{u_1 \cdot (d_1)}{\nu}, \quad Nu = \frac{h \cdot (2d_1 - y)}{k},$$
$$Sh = \frac{h_m \cdot (2d_1 - y)}{D} \quad . \ . \ . \ . \ .(6)$$

Where ν, k and D are kinematics viscosity, thermal conductivity of dry air and mass diffusion coefficient, respectively.

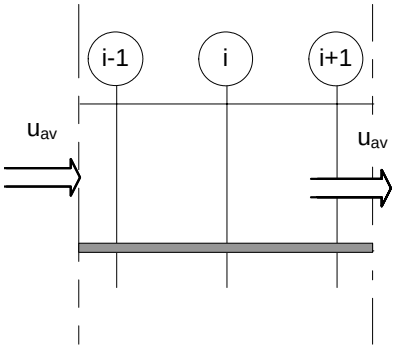

(a) Test section

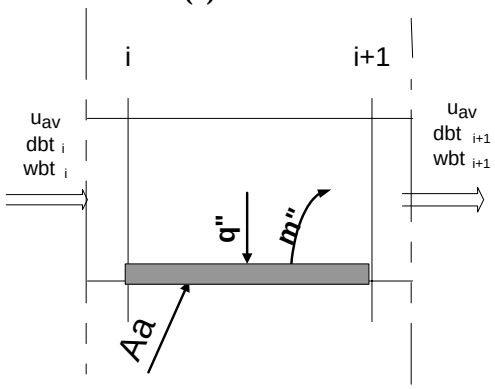

(b) Segment

Figure-3. Measuring positions along test section.

2.3 The carried out measurements

Measurements obtained in this work can be classified into two categories: First one is the temperature measurements and second is the velocity measurements.

2.3.1 Temperature measurements

Thermocouples are used to measure the surface temperature of the test section. Thermocouples are connected to a temperature recorder, which has a 0.1°C sensitive and full-scale range - 100 to 100°C. The used thermocouples are made of copper constant type (K). Two hygrometers are used to measure the dry and wet bulb temperature of humid air. The hygrometers put and move up and down inside the wind tunnel in slots that, the full

scale rang from (-20 to 50°C) the diameter of prob of hygrometer 12mm and length 125 mm.

2.3.2 Velocity measurement

A macro pitot tube meter and Eco series micro-manometer are used to measure the velocity of humid air and water with velocity range from 1 m/sec to 64 m/sec.

These variables are duct dimensions, temperatures, water - and air velocities, which used to calculate the uncertainty in Nusselt number and Reynolds number. The largest calculated uncertainties in the current investigation are less than ±5.5% for Reynolds number and for Nusselt number are less than ±7.8%.

The sets of experimental are preformed during this investigation. The first set in Table-1 involved the flow of humid air over stationary water and the other sets are concerned with the flow of humid air over moving water. The humid aire velocity is varied from 1m/s to 8.4 m/s and the water velocity is varied from 0 to 1.2 m/s.

Table-1. Various cases considered for experimental study.

Case	Velocity ratio β	Air inlet temperature (°C)	Hot water inlet temperature (°C)	Cold water inlet temperature (°C)	Relative humidity in free stream (%)
1	0	21	40	5.5	55
2	0	19	41	4.5	58
3	0	20	40	5.0	59
4	0	19.5	41	4.5	65
5	0.05	23	40	4.5	45
6	-0.05	19	41	5.0	59
7	0.1	24	40	5.0	49
8	-0.1	18	40	4.5	60
9	0.15	20	40	5.5	48
10	-0.15	20	40	5.5	65
11	0.2	22	40	5.0	51
12	-0.2	19	40.5	5.5	68
13	0.3	21	40	4.5	56
14	-0.3	21	40	4.5	70
15	0.3	21.4	40	4	71
16	0.3	20.5	41	4.8	68

3. RESULTS AND DISCUSSIONS

In this section the obtained experimental results are presented and discussed. Accordingly, the experimental results, dry bulb- and wet bulb temperatures, local and average heat transfer, as well as mass transfer coefficients and local, average Nusselt and Sherwood numbers are depicted. Also a comparison between the present results and that of previous available works are also presented in this section.

Figures 4 and 5 shows samples of temperature distribution at different dimensionless longitudinal position (X = 0 to 16). From Figure-4, the dry bulb temperature has minimum value (temperature of water panel) at zero dimensionless vertical distance Z and takes an asymptotic value far from the water panel. The wet bulb temperature takes the same trend of that of the dry bulb temperature as shown in Figure-5. As shown in Figures 4 and 5, dry and wet bulb temperatures decrease in down stream direction.

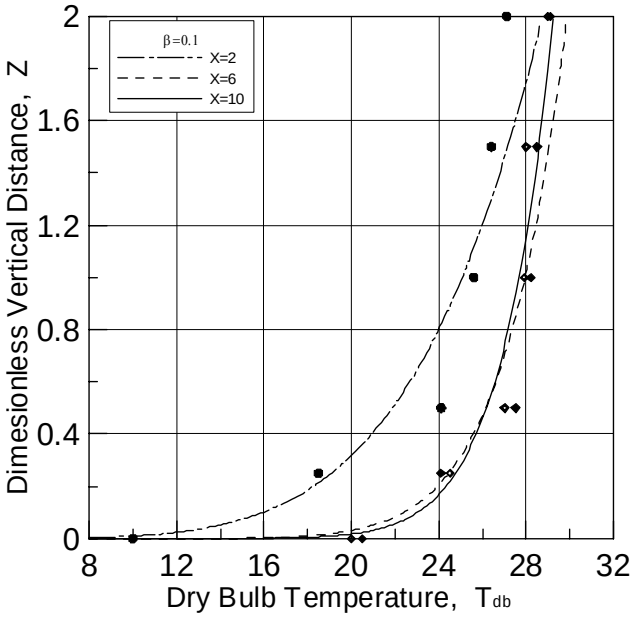

Figure-4. Variation of dry bulb temperature in vertical direction at different values of, X.

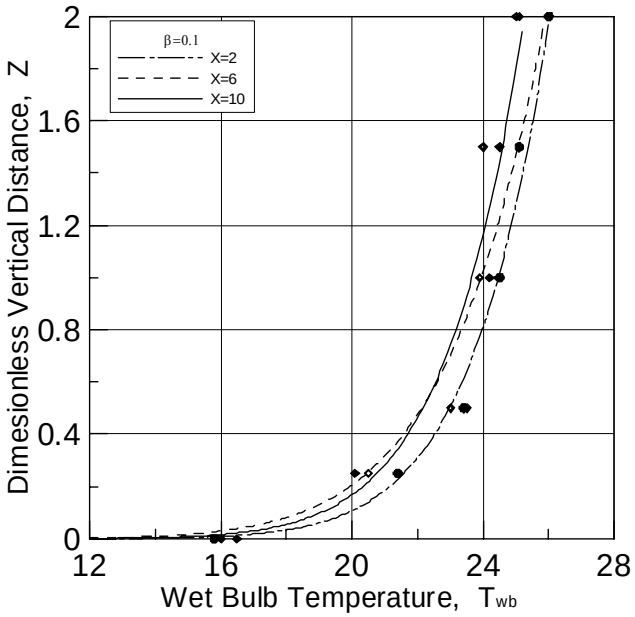

Figure-5. Variation of wet bulb temperature in vertical direction at different values of, X.

Figures 6 and 7 shows the relation between both the local heat and mass transfer coefficients in X-direction at different values of Reynolds number.

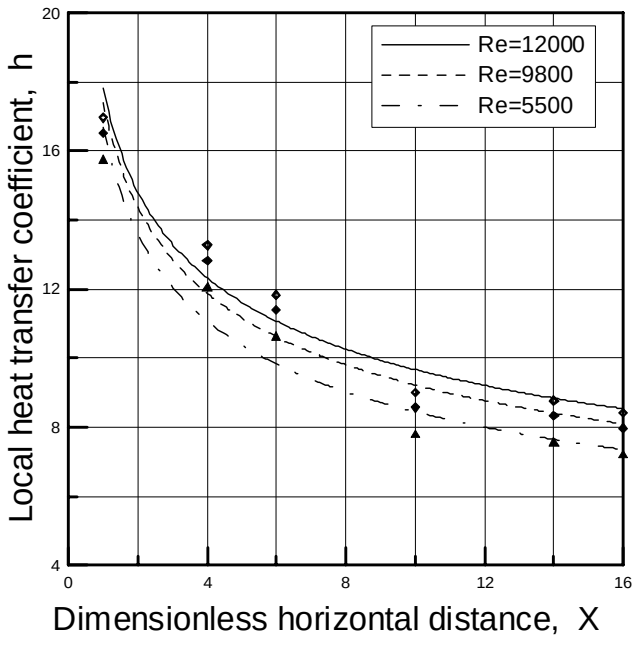

Figure-6. Relation between local heat transfer coefficient for different value of Reynolds number, experimental results.

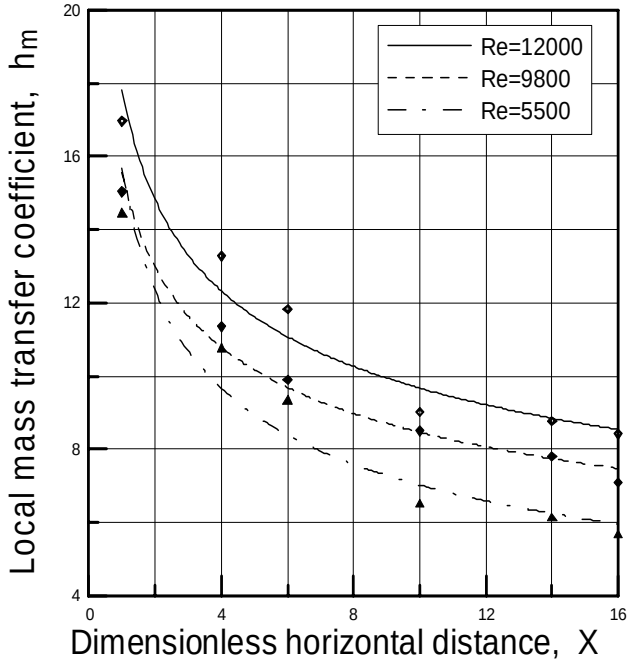

Figure-7. Relation between local mass transfer coefficient for different value of Reynolds number, experimental study.

The local heat transfer coefficient and local mass transfer coefficient, as well, decrease by increasing Reynolds number and increase with increasing Reynolds number.

Figures 8 and 9 shows the variation of average Nusselt number and Sherwood number agaist Reynolds number for different three velocity ratio.

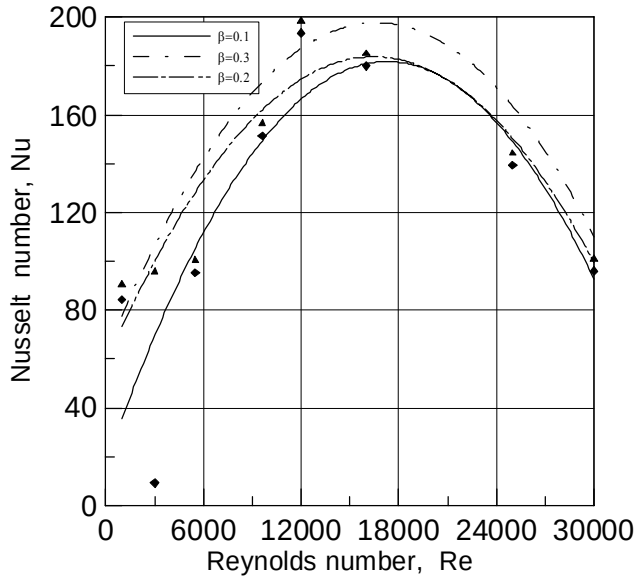

Figure-8. Relation between average Nusselt numbers for different Reynolds number, experimental results.

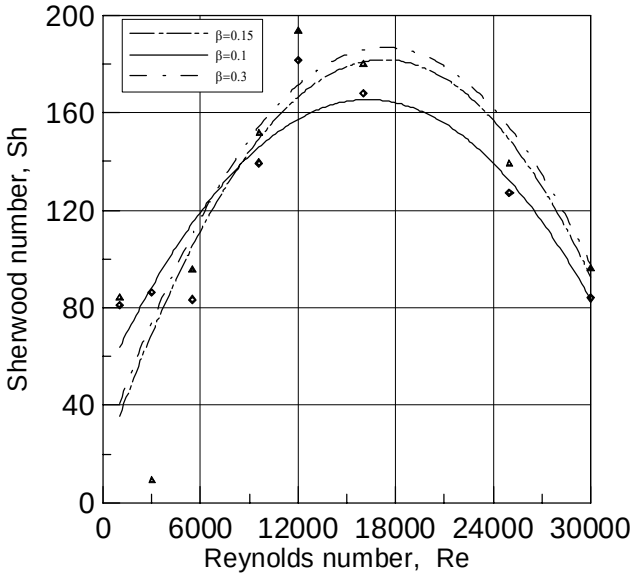

Figure-9. Relation between average Sherwood numbers for different Reynolds number, experimental results.

Average Nusselt and Sherwood numbers against different values of Reynolds number are shown. The average Nusselt and Sherwood numbers increase by increasing Reynolds number up to about Re = 18000, there they have two peaks. Then they decrease with increasing Reynolds number, due to the migration of the water bubble with the moist airflow. Because of this migration, the rate of evaporation, and in turn, rate of heat transfer are decreased.

Figure-10 shows local heat transfer coefficient along the plate of present experimental work and that after reference [8]. As it is clear, both are in good agreement, especially for X > 12.

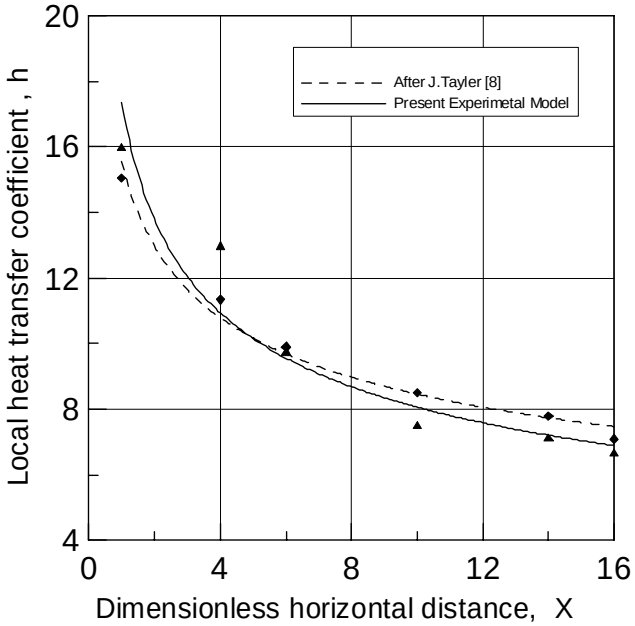

Figure-10. Comparison between local heat transfer coefficient in present and previous work, at Re = 9800 and β = 0.1

4. CONCLUSIONS

In the present study, the evaporation process of water vapor to moist air is, experimentally, analyzed. The effects of process parameters are investigated. These parameters are presented by the following dimensionless physical quantities Prandtl, Schimdt and Reynolds numbers. According to the proposed experimental model, there is an optimum value of Reynolds number, thereafter the increase of flow velocity, and in turn, the Reynolds number cause a decrease of evaporation rate, and in turn, Nusselt and Sherwood numbers. For the present operating conditions, this value of Reynolds number is found to be about 18000. The corresponding values of Nusselt and Sherwood numbers are about 180 and 170, respectively.

The following relations correlate the experimental results, where the Nusselt and Sherwood numbers are expressed as functions of Reynolds, Prandtl and Schmidt numbers:

$$Nu = 1.801\, Re^{0.45}\, Pr^{0.34}\, (1+\beta^{0.24})$$

$$Sh = 1.622\, Re^{0.412}\, Sc^{0.34}\, (1+\beta^{0.3})$$

The range of Reynolds number from 1000 to 12000 and Prandtl and Schmidt numbers from 0.65 to 0.89.

The carried out comparisons between the present and previous study exhibit a fairly good agreement.

Comparison between the obtained results and the previous works in case of steady flow shows good agreement. Empirical correlation for Nusselt number and Sherwood number are obtained.

Nomenclature:

A	Surface area of water panel	m^2
C	Concentration of water vapor in the flowing air	kg/m^3
C_p	Specific heat at constant pressure	$J/(kg.^{\circ}C)$
D	Diffusion coefficient	m^2/s
d_1	Half the vertical height of the duct	m
h	Heat transfer coefficient	$W/(m^2.^{\circ}C)$
h_m	Mass transfer coefficient	m/s
h_{fg}	Latent heat of vaporization	J/kg
k	Thermal conductivity	$W/(m.^{\circ}C)$
L	Length of water panel	m
$\dot{m}_{air}$	airflow rate	kg/s
$\dot{m}_{ev}$	Evaporation rate	kg/s
m''	Mass flux	kg/m^2
Nu	Nusselt number, $Nu=h(d_1-d)/k$	--
P	Pressure	Pa
Pr	Prandtl number, $Pr= C_p\ \mu /k$	---
Q	Rate of heat transfer	W
q''	Heat flux	W/m^2
Re	Reynolds number, $Re = U\ (d_1-d)/\nu)$	---

RH	Relative humidity	%
Sc	Schmidt number, Sc=ν /D	---
Sh	Sherwood number, Sh=h_m ($2d_1$-y)/D	--
T	Temperature	°C
U	Air velocity,	m/s
y	height of water in the duct	m
Greek symbols		
β	velocity ratio= u_2/u_1	---
ΔT	Temperature difference,	°C
θ	Dimensionless temperature	----
ν	Kinematic viscosity	m^2/s
ρ	Density	kg/m^3
Subscripts		
av	average	
db	dry bulb	
sat	saturation	
1,2	air and water	

REFERENCES

Wel-mon Yan. 1995. Transport phenomena of developing laminar mixed convection heat and mass transfer in inclined rectangular ducts. Int. J. Heat Mass Transfer. 38(15): 2905-2914.

G. GROSSMAN and K. GOMMED. 1997. Heat and mass transfer in film absorption in the presence of non - absorption gases. Int. J. Heat Mass Transfer. 40(15): 3595-3606.

KUAN-TZONG LEE. 1998. Mixed convection heat transfer in horizontal rectangular ducts with wall transpiration effects. Int. J. Heat Mass Transfer. 41(2): 411-423.

Eames I. W., Marr N. J. and Sabir H. 1997. The evaporation coefficient of water: a review. Int. J. Heat and Mass Transfer. 40(12): 2963-2973.

Zheng G. S. Worek W. M. 1996. Method of heat and mass transfer enhancement in film evaporation. Int. J. Heat and Mass Transfer. 39(1): 97-108.

Sheikholeslami R. and Watkinson A. P. 1992. Rate of evaporation of water into superheated steam and humidified air. Int. J. Heat and Mass Transfer. 35(7): 1743-1751.

Sparrow E. M. and Tao W. Q. 1983. Enhanced heat transfer in a flat rectangular duct with stream wise-periodic disturbances at one principal wall. ASME J. Heat Transfer. 105: 851-861.

J. Taylor Beard and C.S. Chen. 1971. Convective Heat ad Mass Transfer from Water Surface. Water resources research center Virginia Polytechnic Institute and State University Blacksburg, Virginia.

Haji M. and Chow L. C. 1988. Experimental measurement of water evaporation rates into air and superheated steam. ASME J. Heat Transfer. 110: 237-242.

Claus Borgnakkeand Richard E. sonntay. 1997. Table of Thermodynamic and transport Properties. John Wiley and sons Inc.